Microbial Cell Factories

RESEARCH

Open Access

Evaluating oleaginous yeasts for enhanced microbial lipid production using sweetwater as a sustainable feedstock

Valériane Malika Keita[1,2†], Yi Qing Lee[3†], Meiyappan Lakshmanan[2,4], Dave Siak-Wei Ow[2], Paul Staniland[5], Jessica Staniland[5], Ian Savill[5], Kang Lan Tee[1], Tuck Seng Wong[1,6,7,8*] and Dong-Yup Lee[3*]

Abstract

Background Yeasts exhibit promising potential for the microbial conversion of crude glycerol, owing to their versatility in delivering a wide range of value-added products, particularly lipids. Sweetwater, a methanol-free by-product of the fat splitting process, has emerged as a promising alternative feedstock for the microbial utilization of crude glycerol. To further optimize sweetwater utilization, we compared the growth and lipid production capabilities of 21 oleaginous yeast strains under different conditions with various glycerol concentrations, sweetwater types and pH.

Results We found that nutrient limitation and the unique carbon composition of sweetwater boosted significant lipid accumulation in several strains, in particular *Rhodosporidium toruloides* NRRL Y-6987. Subsequently, to decipher the underlying mechanism, the transcriptomic changes of *R. toruloides* NRRL Y-6987 were further analyzed, indicating potential sugars and oligopeptides in sweetwater supporting growth and lipid accumulation as well as exogenous fatty acid uptake leading to the enhanced lipid accumulation.

Conclusion Our comparative study successfully demonstrated sweetwater as a cost-effective feedstock while identifying *R. toluroides* NRRL Y-6987 as a highly promising microbial oil producer. Furthermore, we also suggested potential sweetwater type and strain engineering targets that could potentially enhance microbial lipid production.

Keywords Oleaginous yeasts, Microbial oil, Microbial cell factories, Sweetwater, Comparative omics

†Valériane Malika Keita and Yi Qing Lee contributed equally to this work.

*Correspondence:
Tuck Seng Wong
t.wong@sheffield.ac.uk
Dong-Yup Lee
dongyuplee@skku.edu
Full list of author information is available at the end of the article

Graphical abstract

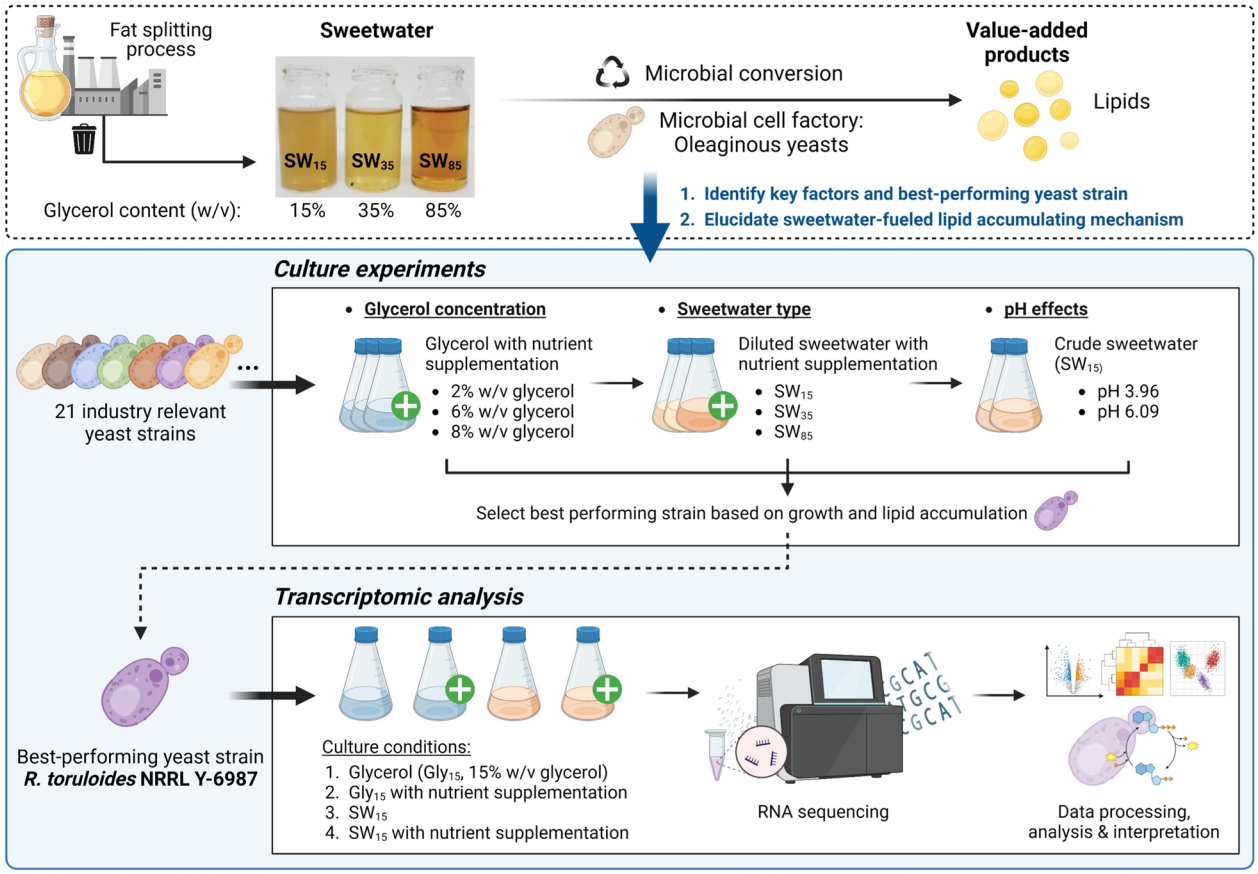

Background

The rapid expansion of the biodiesel industry has flooded the market with high volumes of its by-product, crude glycerol. This endangers the economic viability of biodiesel production and raises a disposal issue. To tackle this challenge, microbial conversion of crude glycerol into value-added chemicals has received a lot of interest due to its alignment with current expectations for sustainability and renewability. In fact, both chemical and biological conversions of crude glycerol are currently under investigation [1, 2]. Notably, the ability of several microorganisms to grow on crude glycerol has been evaluated, resulting in the successful production of various chemicals such as polyols, polyhydroxyalkanoates, organic acids, biogas, biofuels, proteins of industrial relevance, glycerol derivatives and lipids [3]. Among these potential products, lipids are particularly interesting because they could fit into a circular economy [4]. For microbial lipid production, yeasts are notable for their genetic adaptability, versatile carbon utilization, short duplication times and high lipid accumulation potential [5]. Despite extensive research on yeast lipid production, current yields remain suboptimal due to inhibitory effects of methanol [6, 7]. Furthermore, elevated glycerol concentrations also negatively impact cell growth [8]. To overcome these limitations, crude glycerol can be diluted to lower the concentration of impurities and glycerol [9]. Alternatively, feeding strategies during microbial fermentation can be manipulated to increase conversion efficiency [10].

There has been a growing interest in harnessing alternative sources of crude glycerol discharged from fat splitting and saponification processes, which contribute to approximately 30% and 6% of the global glycerol production, respectively [11, 12]. Fat splitting is a process that involves the hydrolysis of food-grade edible oils to generate crude glycerol. Crude glycerol derived from fat-splitting is widely known as sweetwater, has a lower concentration of glycerol (8–20%) and methanol, along with reduced impurities

in comparison to biodiesel-derived crude glycerol [13]. These characteristics suggest that sweetwater might be a more compatible feedstock for lipid production than biodiesel-derived crude glycerol. Furthermore, sweetwater is available in different purity levels: SW_{15} which has glycerol concentration of 15% (w/v) with a low pH and high brownish fatty residue content (Additional file 1: Fig. S1), as well as cleaner forms with glycerol concentrations of 35% (w/v) (SW_{35}) and 85% (w/v) (SW_{85}). SW_{85} is considered a semi-crude glycerol with low economic value of around 0.04–0.09 USD/per pound [14]. Therefore, sweetwater could be more advantageous than biodiesel-derived crude glycerol in terms of efficiency and cost.

To enhance the utilization of sweetwater, we comprehensively evaluated the suitability of sweetwater as a feedstock using 21 selected oleaginous yeast species by comparing both cell growth and lipid accumulation across different glycerol and impurities concentrations, as well as media pH. We observed lipid production induced by sweetwater, and its underlying mechanism was further elucidated through an in-depth analysis of the associated transcriptomic changes.

Results and discussion

Investigating the glycerol tolerance of oleaginous yeasts

21 strains of 17 yeast species (Table 1) which have high industrial potential for lipid production were selected. In the selection of yeast strains for this study, efforts were made to include both well-studied model strains, such as *Yarrowia lipolytica*, *Rhodotorula toruloides*, *Lipomyces starkeyi* and *Rhodotorula glutinis* [15, 16], and relatively less characterized strains including *Barnettozyma californica*, *Cyberlindnera saturnus* and *Lodderomyces elongisporus*. To evaluate strain tolerance to high glycerol concentration, microbiology-grade glycerol which will have no interference from impurities present in sweetwater, was used to cultivate all selected yeast strains. The strains were cultivated in media containing different concentrations of glycerol (2%, 8%, and 16% w/v), supplemented with nutrients using SC mix. These media were denoted as Gly_2SC, Gly_8SC, and $Gly_{16}SC$, respectively, to reflect their glycerol concentration and composition (Table 2, Additional file 1: Figs. S2 and S3). The growth curves obtained were analyzed to derive carrying capacities (CC) and t_{mid}, which represents the maximum population size attained by the available carbon sources and the time required to reach half of the CC, respectively.

All yeast strains demonstrated the ability to utilize Gly_2SC, and some were capable of tolerating Gly_8SC. *T. delbrueckii*, *S. occidentalis*, *W. anomalus*, *R. toluroides* NRRL Y-6987, *S. stipilis* NRRL Y-11545, *S. stipilis* BCC 15191 and *C. xylofermentans* exhibited improved performance in Gly_8SC, achieving a higher final OD_{600} while maintaining a similar growth rate to that observed in Gly_2SC, suggesting that these strains are less susceptible to substrate inhibition. *C. xylofermentans*, *S. occidentalis*, and *T. delbruekii* demonstrated a CC in Gly_8SC 1.5 times higher than that observed in Gly_2SC. However, all strains were unable to achieve higher cell densities in $Gly_{16}SC$, indicating that they were inhibited at high glycerol concentration (Table 2, Additional file 1: Figs. S2 and S3). Despite this, *L. elongisporus*, *M. pulcherrima*, and *R. mucilaginosa* are the most tolerant strains, achieving a similar t_{mid} value for both Gly_2SC and $Gly_{16}SC$. In addition, *T. delbrueckii*, *S. occidentalis* and *R. toluroides* NRRL Y-6987 were also able to produce a final biomass which is comparable to Gly_2SC and Gly_8SC.

Table 1 Strains investigated in this study

No.	Strains (3-letter code)	ID
1	*Barnettozyma californica* (bca)	NRRL Y-1680
2	*Clavispora xylofermentans* (cxy)	BCC 30719
3	*Cutaneotrichosporon curvatus* (ccu)	NRRL Y-1511
4	*Cyberlindnera saturnus* (csa)	NRRL YB-4312
5	*Lipomyces lipofer* (lli)	DSM 70305
6	*Lipomyces starkeyi* (lst)	NRRL Y-1388
7	*Lodderomyces elongisporus* (lel)	NRRL YB-4239
8	*Metschinikowia pulcherrima* (mpu)	NRRL Y-5941-53
9	*Pichia kudriavzevii* (pku)	NRRL Y-7551
10	*Rhodotorula glutinis* (rgl)	NRRL Y-2502
11	*Rhodotorula mucilaginosa* (rmu)	NRRL Y-17283
12	*Rhodotorula toruloides* (rto)	NRRL Y-6987
13	*Rhodotorula toruloides* (rto)	NRRL Y-1091
14	*Scheffersomyces stipitis* (sst)	NRRL Y-7124
15	*Scheffersomyces stipitis* (sst)	NRRL Y-11545
16	*Scheffersomyces stipitis* (sst)	BCC 15191
17	*Schwanniomyces occidentalis* (soc)	NRRL Y-2477
18	*Torulaspora delbrueckii* (tde)	NRRL Y-866
19	*Wickerhamomyces anomalus* (wan)	NRRL Y-366
20	*Yarrowia lipolytica* (yli)	BCC 64401
21	*Yarrowia lipolytica* (yli)	Y203A

Evaluating yeast ability to utilize industrial sweetwater

Next, yeasts were evaluated based on their abilities to utilize sweetwater for growth. Three sweetwater types are available: SW_{15}, SW_{35} and SW_{85}, which were collected from several points along the glycerol refining chain. They have increasing glycerol concentration and purity. Previously, dilution of glycerol-containing discharge from biodiesel manufacturing process with synthetic media was shown to improve microbial growth [9]. However, this is impractical on an industrial scale due to the

Table 2 Strains tolerance to microbiology-grade glycerol

Strains	Gly_2SC [2% (w/v) glycerol]		Gly_8SC [8% (w/v) glycerol]		$Gly_{16}SC$ [16% (w/v) glycerol]	
	t_{mid} (h)	CC	t_{mid} (h)	CC	t_{mid} (h)	CC
B. californica NRRL Y-1680	18.09 ± 4.38	1.47 ± 0.02	17.99 ± 4.72	1.63 ± 0.06	25.98 ± 1.88	1.61 ± 0.04
C. xylofermentans BCC 30719	19.93 ± 0.45	0.92 ± 0.04	33.95 ± 10.95	1.33 ± 0.03	28.5 ± 2.78	1.34 ± 0.05
C. curvatus NRRL Y-1511	21.08 ± 0.29	1.18 ± 0.01	22.93 ± 0.38	1.34 ± 0.02	30.88 ± 2.68	1.16 ± 0.11
C. saturnus NRRL YB-4312	16.45 ± 0.19	1.5 ± 0.02	17.52 ± 0.07	1.78 ± 0.02	22.16 ± 0.99	0.82 ± 0.11
L. lipofer DSM 70305	50.65 ± 13.13	1.17 ± 0.3	77.66 ± 1.26	1.34 ± 0.04	–	–
L. starkeyi NRRL Y-1388	46.8 ± 1.4	1.31 ± 0.01	88.85 ± 0.55	1.55 ± 0.03	–	–
L. elongisporus NRRL YB-4239	27.71 ± 3.96	1.53 ± 0.12	40.43 ± 8.69	1.44 ± 0.22	18.54 ± 0.43	1.67 ± 0.04
M. pulcherrima NRRL Y-5941–53	20.69 ± 2.62	1.48 ± 0.05	18.05 ± 0.05	1.7 ± 0.03	18.52 ± 0.06	1.68 ± 0.02
P. kudriavzevii NRRL Y-7551	22.5 ± 0.83	1.38 ± 0.03	30.73 ± 0.29	1.76 ± 0.06	78.38 ± 8.69	1.72 ± 0.1
R. glutinis NRRL Y-2502	21.14 ± 0.14	1.23 ± 0.04	22.75 ± 0.87	1.42 ± 0.02	–	–
R. mucilaginosa NRRL Y-17283	24.63 ± 3.44	1.46 ± 0.07	26.9 ± 10.2	1.81 ± 0.04	29.63 ± 7.08	1.69 ± 0.03
R. toruloides NRRL Y-6987	23.78 ± 0.32	1.35 ± 0	23.78 ± 0.06	1.84 ± 0.03	73.61 ± 0.54	1.84 ± 0.03
R. toruloides NRRL Y-1091	25.91 ± 3.45	1.35 ± 0.11	24.31 ± 0.54	1.62 ± 0.05	84.08 ± 4.71	1.78 ± 0.1
S. stipitis NRRL Y-7124	22.22 ± 2.29	1.52 ± 0.04	22.57 ± 1.59	1.87 ± 0.03	70.72 ± 1.15	1.73 ± 0.03
S. stipitis NRRL Y-11545	26.35 ± 6.21	1.42 ± 0	29.89 ± 2.1	1.77 ± 0.05	29.89 ± 2.1	1.55 ± 0.05
S. stipitis BCC 15191	20.86 ± 3.71	1.42 ± 0.06	30.03 ± 6.18	1.87 ± 0.05	43.8 ± 4.18	1.82 ± 0.05
S. occidentalis NRRL Y-2477	19.68 ± 3.87	1.07 ± 0.01	19.5 ± 2.94	1.56 ± 0.07	54.37 ± 4.63	1.56 ± 0.03
T. delbrueckii NRRL Y-866	17.93 ± 2.41	0.91 ± 0.03	18.2 ± 0.09	1.42 ± 0.06	43.48 ± 2.44	1.44 ± 0.04
W. anomalus NRRL Y-366	16.6 ± 0.08	1.54 ± 0.03	17.85 ± 0.02	1.89 ± 0.02	19.35 ± 0.28	1.84 ± 0.02
Y. lipolytica BCC 64401	20.78 ± 0.94	1.46 ± 0.09	19.48 ± 0.02	1.74 ± 0.02	23.09 ± 1.17	1.82 ± 0.04
Y. lipolytica Y203A	17.29 ± 0.4	1.52 ± 0.07	17.1 ± 0.17	1.74 ± 0.03	17.82 ± 0.1	1.62 ± 0.07

associated increase in production cost. Hence, the use of SW_{15}, the crudest form of sweetwater with a relatively lower concentration of glycerol without prior dilution is preferable in terms of cost. Conversely, although SW_{35} and SW_{85} offer advantages such as higher purity and lower moisture levels, rendering them an extended shelf life, dilution and/or nutrient addition prior use is necessary due to their higher glycerol concentration.

SW_{15}, SW_{35} and SW_{85} were supplemented with SC mix to produce media with a final glycerol content of 1.5% (w/v), referred to as $SW_{15>1.5}SC$, $SW_{35>1.5}SC$ and $SW_{85>1.5}SC$, respectively. We first compared the suitability of these three media for yeast cultivation. For most yeast strains, growth profiles were similar regardless of how the diluted sweetwater was prepared. Additionally, the growth profiles of all yeast strains in these media were highly similar to that of Gly_2SC (Table 2, Additional file 1: Figs. S2 and S3). For simplicity, $SW_{15>1.5}SC$, $SW_{35>1.5}SC$ and $SW_{85>1.5}SC$ were collectively referred to as $SW_{1.5}SC$, and this medium served as a reference medium throughout this study. Next, we evaluated the growth of all 21 strains in SW_{15} and $SW_{1.5}SC$, to identify differences resulting from sweetwater dilution and/or nutrient supplementation, noting that SW_{15} is the crudest form of sweetwater without any nutrient supplementation (Table 3, Additional file 1: Fig. S4). To our surprise, all 21 strains were able to grow in SW_{15} despite its high glycerol concentration, including *L. lipofer* and *L. starkeyi* which were unable to grow in $Gly_{16}SC$, potentially suggesting the presence of other preferred carbon sources in sweetwater. In comparison to SW_{15}, we observed a slightly higher OD_{600} in $SW_{1.5}SC$, suggesting that nutrient supplementation together with a lower glycerol concentration is more favorable for yeast growth. Nevertheless, we can confirm that SW_{15} is suitable for yeast growth without nutrient supplementation. In fact, the composition of SW_{15} enhanced the growth of some yeast strains. *R. glutinis* showed slow growth in $Gly_{16}SC$ but achieved one of the highest biomasses in SW_{15}. *R. mucilaginosa* and *R. toruloides* NRRL Y-6987 growth rates were also improved in SW_{15}, but their carrying capacities decrease, indicating that SW_{15} initially offered an environment more favorable for proliferation, but later turned inhibitory possibly due to low initial pH of SW_{15} (pH 3.95) or depletion of nutrients.

To further explore optimal growth conditions, we formulated an additional media using SW_{15} by adjusting its pH from 3.95 to 6.09. Previous research suggested that pH adjustments can affect yeast growth in glycerol [17, 18]. However, we found that the average growth

Table 3 Effects of glycerol concentration and pH of sweetwater on yeast growth

Strains	Concentration effect				pH effect			
	$SW_{35>1.5}SC$		$SW_{35}SC$		SW_{15} pH 6.09		SW_{15} pH 3.95	
	t_{mid} (h)	CC	t_{mid} (h)	CC	t_{mid} (h)	CC	t_{mid} (h)	CC
B. californica NRRL Y-1680	9.45 ± 0*	1.4 ± 0*	19.75 ± 0.08	1.62 ± 0.01	21.23 ± 0.57	1.05 ± 0.04	22.68 ± 2.85	1.05 ± 0.02
C. xylofermentans BCC 30719	23.7 ± 1.82	0.96 ± 0.08	60.82 ± 4.33	1.91 ± 0.04	39.67 ± 2.92	1.2 ± 0.03	49.2 ± 6.36	0.99 ± 0.11
C. curvatus NRRL Y-1511	21.26 ± 1.15	1.46 ± 0.01	64.98 ± 2.76	1.42 ± 0.01	41.53 ± 0.88	1.24 ± 0.04	93.65 ± 8.76	1.29 ± 0.24
C. saturnus NRRL YB-4312	13.43 ± 2.48	1.45 ± 0.03	26.13 ± 0.73	1.68 ± 0.04	29.25 ± 0.45	1.32 ± 0.02	31.29 ± 0.48	1.29 ± 0.02
L. lipofer DSM 70305	59.51 ± 3.32	0.89 ± 0.09	171.86 ± 27.74	0.69 ± 0.25	79.73 ± 4.38	0.8 ± 0.05	66.07 ± 3.93	0.35 ± 0.06
L. starkeyi NRRL Y-1388	47.11 ± 0.56	0.99 ± 0.02	-	-	66.81 ± 1.62	0.75 ± 0.04	67.86 ± 1.22	0.59 ± 0.06
L. elongisporus NRRL YB-4239	18.34 ± 0.08	1.33 ± 0.03	35.9 ± 3.4	1.85 ± 0.02	21.51 ± 0.95	1.08 ± 0.1	19.88 ± 0.18	1.15 ± 0.02
M. pulcherrima NRRL Y-5941-53	19.11 ± 0.18	1.38 ± 0.01	38.26 ± 0.28	1.67 ± 0.01	19.83 ± 0.09	1.41 ± 0.01	20.24 ± 0.17	1.42 ± 0.02
P. kudriavzevii NRRL Y-7551	22.13 ± 0.42	1.3 ± 0.02	36.96 ± 2.06	1.54 ± 0.01	27.56 ± 5.35	0.87 ± 0.26	54.06 ± 16.75	0.73 ± 0.11
R. glutinis NRRL Y-2502	24.18 ± 0.27	1.26 ± 0.02	103.3 ± 4.95	1.54 ± 0.03	27.18 ± 0.72	1.29 ± 0.03	54.23 ± 1.99	1.32 ± 0.02
R. mucilaginosa NRRL Y-17283	20.03 ± 0.07	1.3 ± 0.01	22.38 ± 0.1	1.67 ± 0.02	20.6 ± 0.37	1.1 ± 0.03	23.85 ± 0.97	1.02 ± 0.02
R. toruloides NRRL Y-6987	23.03 ± 1.76	1.57 ± 0.05	35.37 ± 0.23	1.73 ± 0.03	21.74 ± 0.35	1.34 ± 0.03	28.07 ± 1.83*	1.28 ± 0.02*
R. toruloides NRRL Y-1091	21.48 ± 0.62	1.35 ± 0.02	55.84 ± 0.66	1.78 ± 0.03	24.06 ± 1.75	1.15 ± 0.05	42.43 ± 2.47	1.13 ± 0.04
S. stipitis NRRL Y-7124	20.1 ± 0.61	1.45 ± 0	139.16 ± 0.64	1.82 ± 0.05	28.12 ± 6.3	1.3 ± 0.05	21.68 ± 1.7	1.08 ± 0.07
S. stipitis NRRL Y-11545	19.44 ± 1.13	1.35 ± 0.05	37.01 ± 0.43	1.76 ± 0.02	21.27 ± 0.32	1.23 ± 0.03	23.87 ± 2.81	1.09 ± 0.04
S. stipitis BCC 15191	23.76 ± 0.62	1.28 ± 0.02	33.69 ± 1.95	1.73 ± 0	20.71 ± 0.18	1.26 ± 0.03	21.18 ± 0.63	1.17 ± 0.1
S. occidentalis NRRL Y-2477	19.38 ± 0.24	1.12 ± 0.05	24.21 ± 0.09	1.73 ± 0.03	33.83 ± 1.08	1.45 ± 0.01	49.01 ± 1.93	1.24 ± 0.03
T. delbrueckii NRRL Y-866	18 ± 0.3	0.81 ± 0.06	26.64 ± 0.34	1.65 ± 0.04	21.56 ± 1.06	1.02 ± 0.06	21.09 ± 0.95	0.57 ± 0.07
W. anomalus NRRL Y-366	13.71 ± 1.88	1.37 ± 0.04	122.47 ± 3.04	1.98 ± 0.03	20.27 ± 0.07	1.41 ± 0.01	21.74 ± 0.35	1.84 ± 0.02
Y. lipolytica BCC 64401	20.43 ± 1.42*	1.39 ± 0*	19.99 ± 0.12	1.83 ± 0.03	21.59 ± 1.03	1.21 ± 0.04	20.75 ± 0.12	1.32 ± 0.01
Y. lipolytica Y203A	17.27 ± 1.52*	1.45 ± 0.05*	18.31 ± 0.32	1.69 ± 0.01	32.84 ± 10.87	1.33 ± 0.01	19.78 ± 0.3	1.32 ± 0.02

All the associated growth curves are available in Additional file 1: Figs. S6 and S7. An asterisk (*) indicates averages computed with less than 4 replicates

rate of the strains was not significantly different at both pH values, although certain individual differences were observed (Table 3, Additional file 1: Fig. S5). Specifically, *R. glutinis* NRRL Y-2502, *R. toruloides* NRRL Y-1091, *C. curvatus*, *T. delbrueckii*, and *S. occidentalis* performed better in pH 6.09, while *Y. lipolytica* (BCC 64401 and Y203A) strains slightly favored low pH. Overall, in both pH conditions, *W. anomalus*, *M. pulcherrima*, and *Y. lipolytica* (BCC 64401 and Y203A) exhibited the enhanced carrying capacities and growth rates, indicating that they are potential yeast candidates for sweetwater utilization. Since growth differences in two pH conditions were minor, we can infer that nutrient limitation is the limiting factor for yeast growth in SW_{15}.

Assessing lipid production of 21 strains grown in SW_{15} and $SW_{1.5}SC$

We next compared the lipid production of 21 strains in SW_{15} by cultivating them in tubes. To address the nutrient limitation in SW_{15}, we also included $SW_{1.5}SC$. Furthermore, taking into consideration the varying growth rates of different strains and the coupling of lipid accumulation to growth phase, we analyzed the cellular lipid content after 3 and 10 days of cultivation. Based on average fluorescence signals across the 4 samples (SW_{15} 3 days, SW_{15} 10 days, $SW_{1.5}SC$ 3 days, $SW_{1.5}SC$ 10 days), we found that the best lipid accumulators are *R. toluroides* NRRL Y-6987, *L. starkeyi*, *R. glutinis*, *C. saturnus* and *L. elongisporus* (Fig. 1a–d). Notably, some strains had higher lipid accumulation in SW_{15}. For instance, *R. mucilaginosa*, *S. stipitis* NRRL Y-7124, *M. pulcherrima* and *C. saturnus* accumulated more lipids in SW_{15} in comparison to $SW_{1.5}SC$ on average, suggesting that these strains better accumulate lipids under low nutrient conditions and/or high C/N ratio. Important to highlight, nutrient supplementation will also likely reduce the C/N ratio. On the other hand, *W. anomalus*, *Y. lipolytica* (BCC 64401 and Y203A) and *M. pulcherrima* showed relatively low lipid accumulation, despite growing best in sweetwater.

Taken together, growth in SW_{15} despite of a different pH (Table 3 and Additional file 1: Fig. S5) suggests the presence of essential nutrients including carbon and nitrogen sources required for yeast growth. This is consistent with previous findings indicating that sweetwater contains glycerol, matter organic

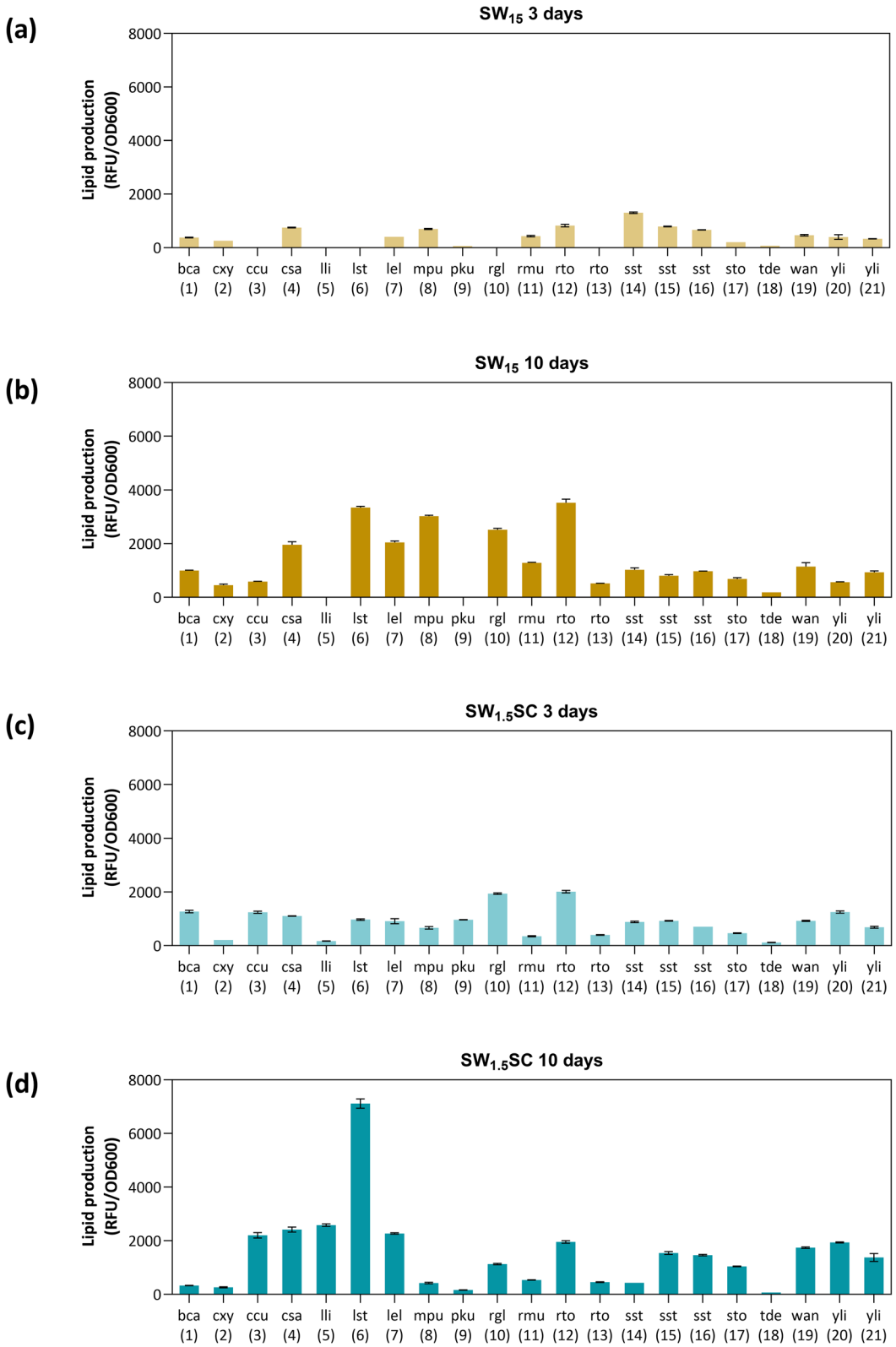

Fig. 1 Lipid production of 21 investigated strains grown in tubes using sweetwater-based media. Lipid production of the 21 investigated strains in **a** SW_{15} on day 3, **b** SW_{15} on day 10, **c** $SW_{1.5}SC$ on day 3 and **d** $SW_{1.5}SC$ on day 10. Error bars denote the standard deviations. 3-letter codes are abbreviations for full species names which can be found in Table 1

non-glycerol (MONG) which comprises of entrained fatty matters (e.g., free fatty acids, fatty acid methyl esters, diglycerides, monoglycerides, and unprocessed oil) and other organic components (e.g., proteins), as well as ash and moisture [19]. However, the higher lipid accumulation in SW_{15} compared to $SW_{1.5}SC$ may indicate a limitation in nitrogen source. Nitrogen limitation is reported to reduce the intracellular levels of adenosine monophosphate (AMP) [20], thereby inhibiting isocitrate dehydrogenase in the Krebs cycle which induces accumulation of citrate in mitochondria, which is then exported to the cytoplasm for acetyl-CoA production through citrate lyase (ACL) [21]. In some yeasts, citrate accumulation is known to initiate fatty acid synthesis by activation of acetyl-CoA carboxylase [22]. Furthermore, impurities in sweetwater including free fatty acids, monoacylglycerol, diacylglycerol and triacylglycerol can function as a secondary carbon source or add to the intracellular lipid pool, thereby contributing to growth or lipid accumulation. Notably, hydrophobic substrates have been reported to be utilized by *C. curvatus*, *R. toruloides* and *Y. lipolytica* [6, 23, 24]. Given SW_{15}'s ability to promote lipid accumulation, potential strategies for improvement could involve optimizing feeding approaches or enhancing strain tolerance to high glycerol concentrations through adaptive laboratory evolution, aiming to boost cell densities in SW_{15} [3].

Since *R. toluroides* NRRL Y-6987 had the highest lipid accumulation in sweetwater-based medium, we proceeded to verify their growth and sweetwater-induced lipid accumulation abilities through time-course monitoring at a larger scale cultivation using flask cultures. We observed that growth curves of *R. toluroides* NRRL Y-6987 were significantly different in SW_{15} and $SW_{1.5}SC$ (Fig. 2a).

Lipid accumulation difference is also clearly visible on TLC (Fig. 2b). Furthermore, maximum normalized fluorescence signals recorded for *R. toluroides* NRRL Y-6987 in SW_{15} is 7.1× higher than that in $SW_{1.5}SC$, demonstrating that its lipid accumulation is better induced by lower nutrient conditions and/or higher C/N ratio in SW_{15} (Fig. 2c, d). Taken together, this indicates that nutrient supplementation or dilution is not necessary for lipid accumulation. From an industrial application perspective, SW_{15} can be directly used for microbial fermentation for lipid production without pre-processing. Notably, a decline in lipid content can be observed around the 200-h mark in SW_{15}. This reduction points to lipid degradation prompted by carbon depletion, a phenomenon commonly observed in oleaginous yeasts that utilize stored lipids as an energy source under carbon-starved conditions, typically during later stages of sampling [25, 26]. This suggests that strategies including harvesting cells prior to lipid degradation, gene knockout targeting the responsible lipid degradation genes, or maintaining a consistent carbon source supply [27] can be employed to enhance lipid yield.

Exploring the transcriptomic changes related to sweetwater utilization by *R. toruloides* NRRL Y-6987

To elucidate the mechanism underlying sweetwater-induced lipid accumulation, we formulated four different media using sweetwater or microbiology-grade glycerol, each with or without nutrients, respectively named SW_{15}, $SW_{1.5}SC$, Gly_{15} and $Gly_{1.5}SC$. Next, RNA from *R. toruloides* NRRL Y-6987 grown in these four media was extracted and sequenced, followed by analysis of the transcriptomic changes (see "Materials and methods"). Principal component analysis (PCA) showed clear separation between the conditions and the close clustering of the biological replicates of each condition. PCA also confirmed that the predominant factor driving the observed differences was nutrient availability, as the first principal component (PC1) accounted for 60.4% of the total variation observed and clearly separated samples in media with or without supplementation of nutrients (Fig. 3a). Next, the second principal component (PC2) which explains 17.4% of the variations clearly separated the transcriptomes of samples from sweetwater and microbiology-grade glycerol. This is observed from projection on PC2 which produced the greatest distance between $Gly_{1.5}SC$ and $SW_{1.5}SC$. The third principal component (PC3) which accounts for 11.5% of the differences also represents the differences between microbiology-grade glycerol and sweetwater (Fig. 3b), evidenced by SW_{15} and Gly_{15} transcriptomes which clustered furthest away from each other. These results indicate that supplementation of nutrients, followed by the source of glycerol, are key factors for transcriptomic changes.

Next, all genes were categorized into 24 functional groups and their contributions to each category to PC1, PC2 and PC3 was computed (Fig. 3c). We found that genes contributing the most to PC1, PC2 and PC3 are in the categories of "Unknown function", "Carbohydrate transport and metabolism", "Secondary metabolites metabolism and transport", "Energy production and conversion", "Inorganic ion transport and metabolism" and "Lipid transport and metabolism". Prevalence of genes with unknown functions highlights the importance of characterizing unconventional yeasts. Even so, we can infer that metabolism and transport of carbohydrates, secondary metabolites and inorganic ions are most affected by nutrient availability. Important to note, SC nutrient mix enriches the

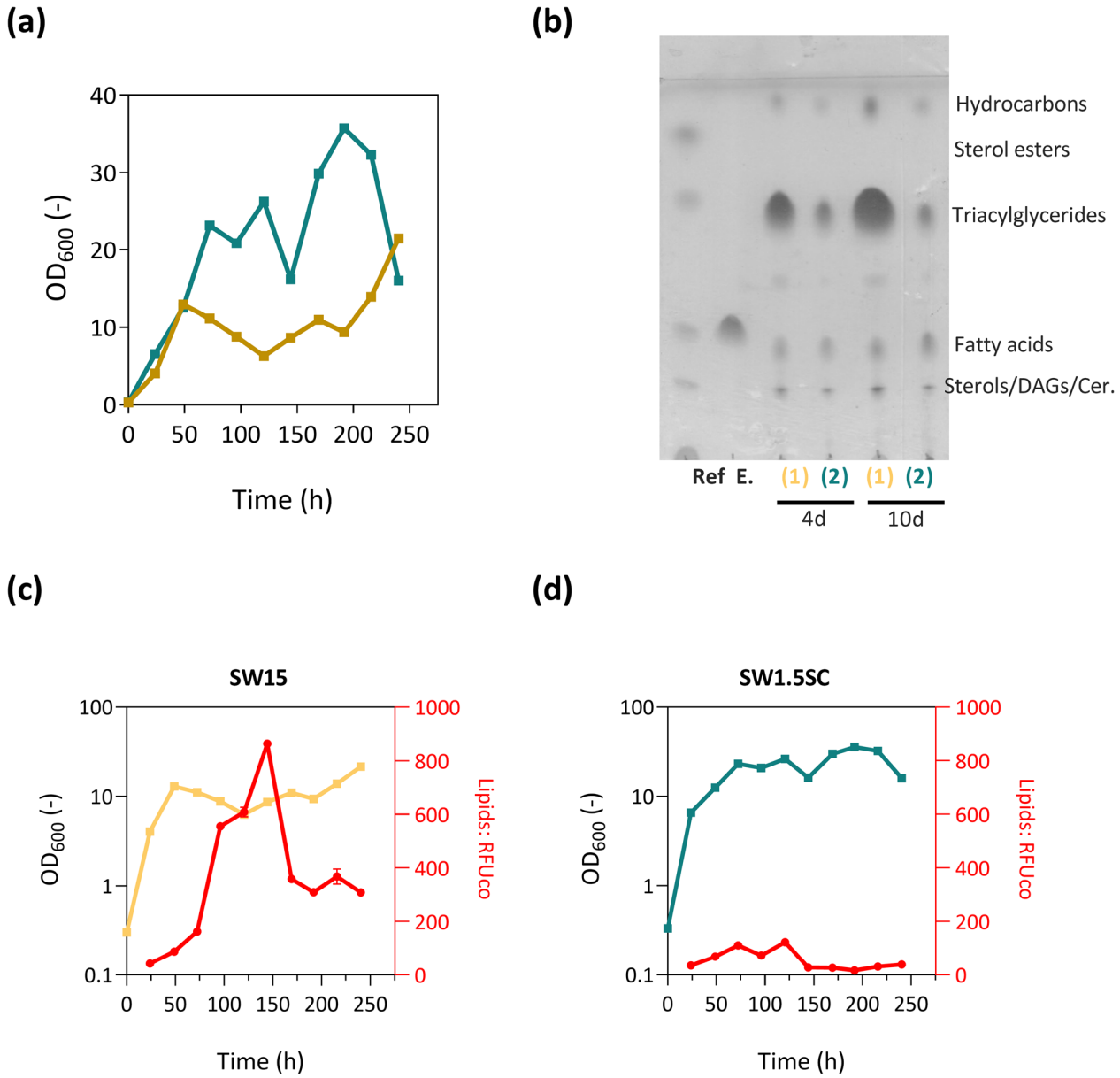

Fig. 2 Growth and lipid production of *R. toluroides* NRRL Y-6987 in flask cultures. **a** Comparison of *R. toluroides* NRRL Y-6987 growth in different media. **b** Comparison of *R. toluroides* NRRL Y-6987 lipid accumulation profiles in different media. **c**, **d** Lipid content over time. OD_{600} were plotted on a logarithmic scale for improved visualization. Fluorescence of the stained cells was measured in quadruplicate and subsequently normalized by the OD_{600} of each sample, resulting in RFU/OD_{600} values

growth media with essential amino acids, nitrogenous bases, inorganic ions, and vitamins, and therefore may cause gene expression changes in the relevant gene categories. For example, inorganic ion transport and metabolism contributed significantly to PC1. On the other hand, genes involved in energy and lipid metabolism contribute more to PC3, suggesting major differences in related pathways when cells are grown in sweetwater as compared to microbiology-grade glycerol. "Lipid metabolism and transport" contains genes involved in lipid biosynthesis and degradation, as well as lipid modification and mobilization. Additional observations on the globally low contribution of the category "cell wall/membrane/envelope biogenesis" suggests that the high contribution of lipid metabolism is mainly due to their involvement in signaling processes and lipid storage instead of involvement in membrane biogenesis/modification.

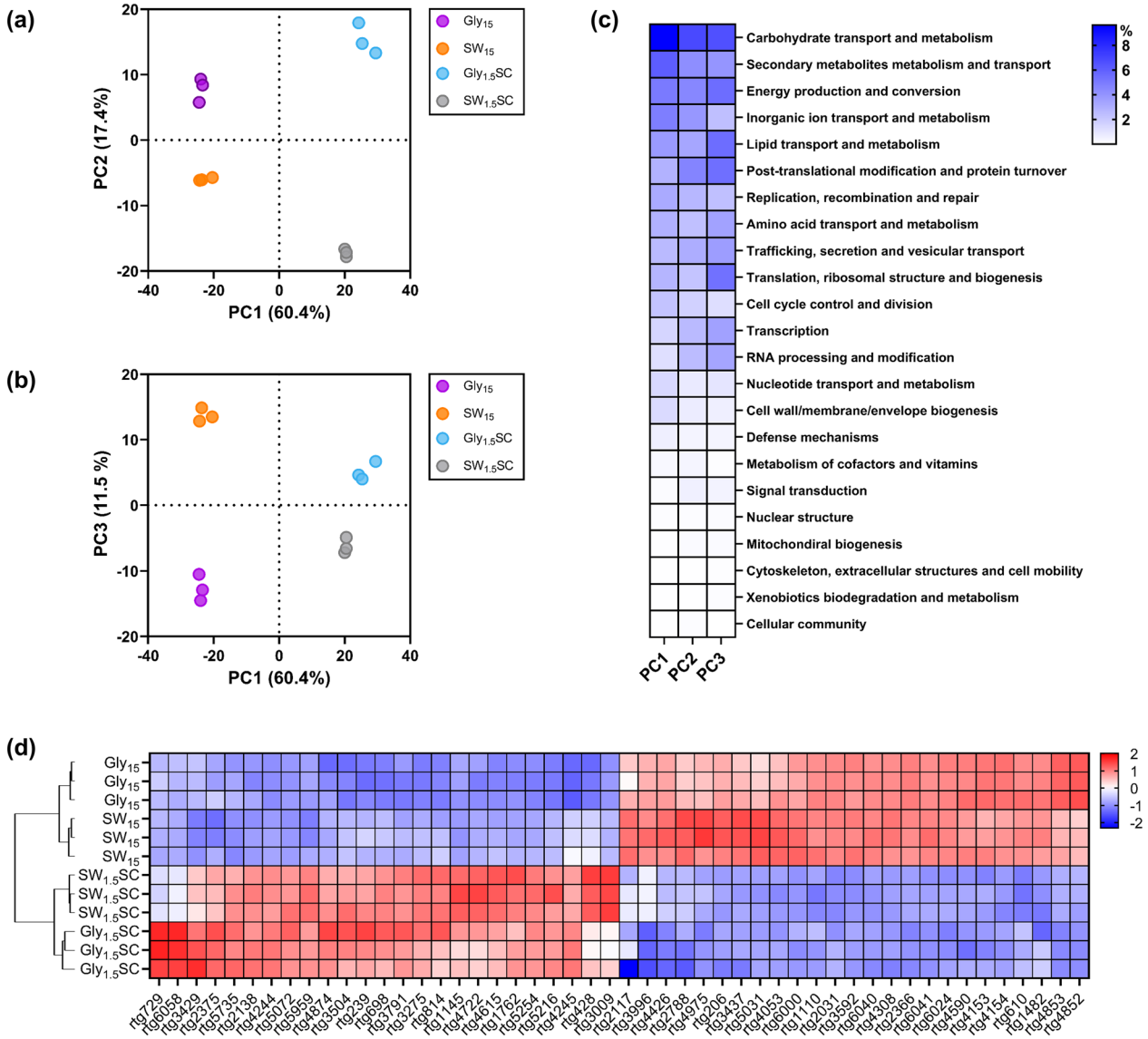

Fig. 3 Comparison of *R. toruloides* NRRL Y-6987 transcriptomes in 4 media. **a**, **b** PCA score plots of transcriptomes in Gly_{15}, SW_{15}, $Gly_{1.5}SC$ and $SW_{1.5}SC$. **c** Functional categories were sorted by descending contribution. To improve visibility, genes with unknown functions were excluded from the heatmap. **d** Heatmap showing normalized expression counts of the top 50 annotated genes which contributes the most to PC1-3

Hierarchical clustering confirmed that *R. toluroides* cultivated in sweetwater and glycerol media exhibited different transcriptomic responses (Fig. 3d and Additional file 1: Fig. S8). To identify the genes behind the transcriptomic changes associated with nutrient availability and glycerol type, we analyzed the top 50 functionally annotated genes contributing the most to PC1, PC2 and PC3. Hierarchical clustering was performed on the z-scores of normalized gene expression of the top 50 genes to visualize genes with high inter-replicate variability (Fig. 3d). We found that, for a given condition, gene expression across replicates was highly consistent, which is coherent with the close clustering among biological replicates observed in PCA, validating the quality and consistency of our data. Next, we compared expression levels of the top 50 genes to investigate the variances between two experimental conditions: (1) absence of nutrient addition and high glycerol concentration (SW_{15} and Gly_{15}) and (2) nutrient addition with low glycerol concentration ($SW_{1.5}SC$ and $Gly_{1.5}SC$).

We observed that genes involved in carbohydrate transport and metabolism, namely *rtg3791* (chitinase), *rtg1145* (TNA1), *rtg1762* (HXT), *rtg5254* (HXT), *rtg4244*

(MAL31), *rtg4245* (IMA1), *rtg4615* (ecfuP), and *rtg4722* (JEN1) are more expressed in the presence of nutrients at low glycerol concentrations (Fig. 3d). Since the cell wall of *R. toruloides* contains chitin [28], *rtg3791* likely contributes to cell wall remodeling activities. Remaining genes can be identified as proton symporters for hexoses (*rtg1762* and *rtg5254*), maltose (*rtg4244*), fucose (*rtg4615*) and carboxylic acids (*rtg4722*) (Additional file 1: Table S1), while JEN1 is a lactate transporter induced by non-fermentable carbon sources including glycerol, derepressed by glucose absence in *S. cerevisiae* [29]. Interestingly, expression of JEN1 is dependent on the kinase SNF1 [29], which connects various pathways involved in stress regulation including TORC pathway for nitrogen sensing, RTG2/SNF3 pathway for glucose sensing, PKA pathway for general stress response and HOG1 pathway for osmotic shock. Next, most lipid metabolism genes with high contribution to PC1 to PC3 are putatively involved in lipid degradation and modification, such as acyl-CoA dehydrogenase (*rtg5959*), peroxisomal MaoC dehydratase (*rtg2138*), and peroxisomal 2,4-dienoyl-CoA reductase (*rtg206*). Since acyl-CoA dehydrogenase is involved in β-oxidation, this may suggest that β-oxidation is more active in the presence of nutrients at low glycerol concentration (Additional file 1: Table S1).

Comparing Gly_{15} and SW_{15} which both have no nutrient addition and high glycerol concentration, genes related to ion transport highly contributes to the PCs, in particular *rtg6000* (ammonium transporter, Amt family) which is involved in NH_4^+/NH_3 uptake (Fig. 3d and Additional file 1: Table S1). Notably, *rtg6000* which was upregulated in SW_{15} is homologous to three endogenous scMEP proteins of *S. cerevisiae* and shares the highest identity with scMEP2, an ammonium sensor which induces pseudohyphal growth during ammonium limitation [30]. scMEP genes encode ammonia permeases and are highly upregulated after exhaustion of a preferred nitrogen source or in presence of non-preferred source [31]. These genes are also related to nitrogen catabolite repression which allows selection of the optimal nitrogen source for growth [32]. This suggests that SW_{15} and Gly_{15} differ in their nitrogen composition.

Additionally, differences in stress-related response can also be observed between the transcriptomes. Notably, rtg4659, a heat shock transcription factor (HSF1), which is also a general stress effector, has elevated expression in sweetwater as compared to Gly_{15}/$Gly_{1.5}$SC, but similar expression levels between Gly_{15} and $Gly_{1.5}$SC, as well as between SW_{15} and $SW_{1.5}$SC. This indicates that sweetwater can trigger non-nutrient related stress responses even when it is diluted. For example, there may be pH-induced transcriptomic changes as sweetwater is originally acidic (in our case, pH 3.95 of SW_{15}). While pH was not specifically controlled in this experiment due to the confirmed insensitivity of *R. toluroides* NRRL Y-6987 to pH changes as indicated in Table 3 and Additional file 1: Fig. S5, further investigations into the potential pH-induced transcriptomic changes in sweetwater could provide valuable insights in future studies. Taken together, *R. toruloides* NRRL Y-6987 responses to the change of growth environment by adjusting primarily its carbohydrate, inorganic ion, and lipid metabolism.

Comparative analysis for SW_{15} and Gly_{15}

To understand more about the transcriptomic differences between SW_{15} and Gly_{15} and investigate possible mechanisms underlying sweetwater-induced lipid accumulation, a second analysis was performed by focusing only on the relevant transcriptomes. Growth is improved substantially in SW_{15} in comparison to Gly_{15} (Additional file 1: Fig. S9). 72.92% of the difference between the two conditions can be captured by PC1 while other PCs mainly describe inter-replicate differences (Fig. 4a, b). The contribution of each functional category, in addition to the top 50 annotated genes contributing the most to PC1 were analyzed (Fig. 4c, d).

Our data and analysis hinted the presence of nitrogen sources in SW_{15}. *rtg4852* and *rtg4853*, respectively annotated as nitrate/nitrite transporter and nitrite reductase, were highly expressed in Gly_{15} (Figs. 4c and 5). *rtg4853* shares homology with umNAR1 from *Ustilago maydis* and ncNIT-6 from *Neurospora crassa*, genes which are known to be influenced by nitrogen metabolite repression, and are triggered by the absence of ammonia or presence of nitrate [33, 34]. On the other hand, in SW_{15}, the low expression of *rtg4853* suggests the presence of ammonium or nitrogen source in SW_{15}. Oligopeptides may be a possible nitrogen source, indicated by increased expression of *rtg3315* and *rtg5673* which are oligopeptide transporters. Furthermore, upregulation of *rtg6000* which encodes an ammonium transporter and the amidase *rtg3792* which facilitates ammonium production from arginine, tryptophan and phenylalanine implies the digestion of exogenous oligopeptides and subsequent processing of resulting amino acids (Fig. 5 and Additional file 1: Table S2). Additionally, *rtg5216* (ubiquitin C) expressing 5-times more in SW_{15} further supports that *rtg3792* is metabolizing amino acids, leading to differences in protein turnover/autophagy.

Conversely, when nitrogen is limited, citrate is accumulated as a result of a less active Krebs cycle. Excess citrate is then directed into fatty acid synthesis. Later, acetyl-CoA is produced from citrate through ACL, then converted into malonyl-CoA by acetyl-CoA carboxylase (ACC). These two enzymes, along with

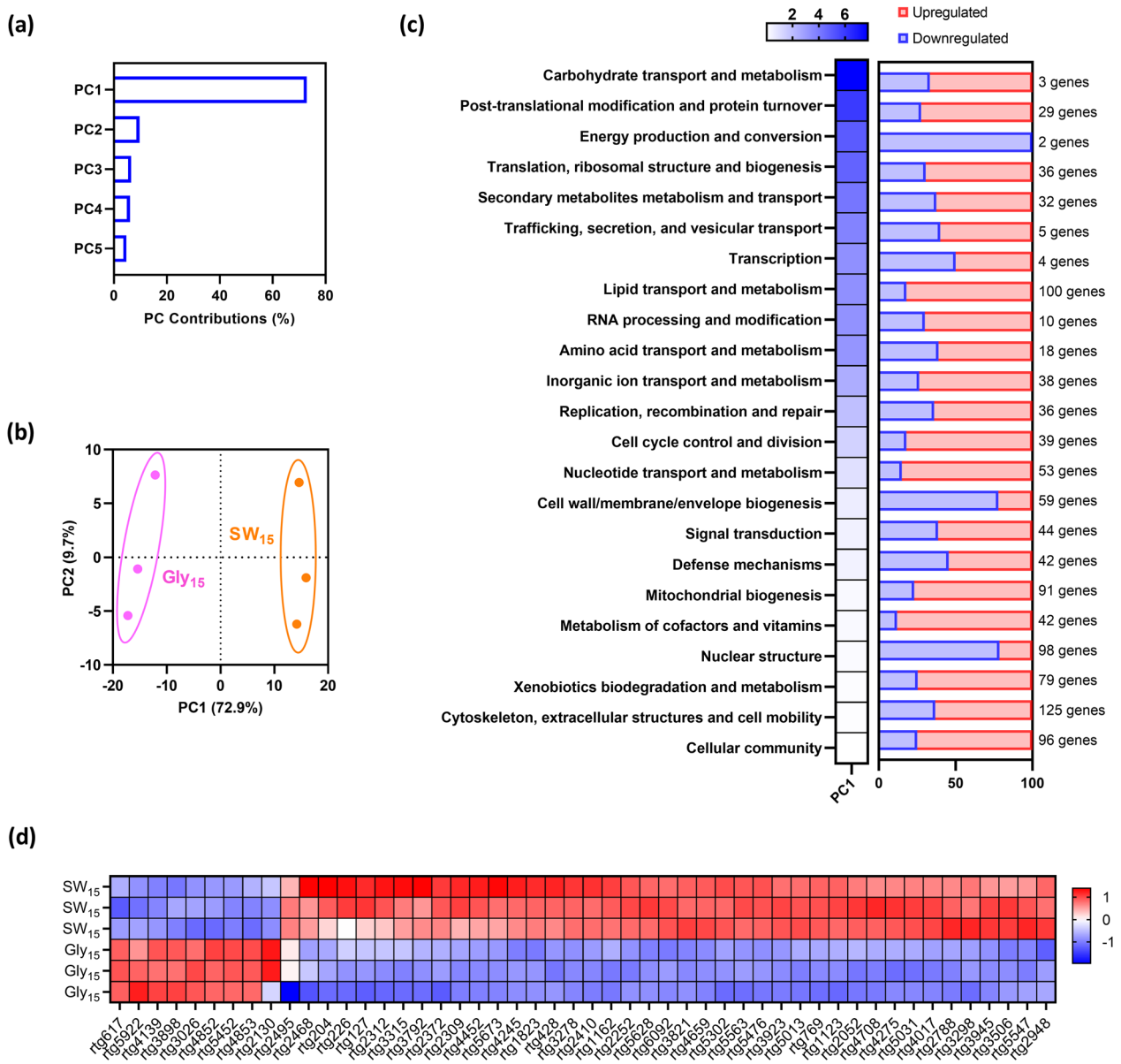

Fig. 4 Comparison of *R. toruloides* NRRL Y-6987 transcriptome in SW_{15} and Gly_{15}. **a** Scree plot shows the percentage of variance explained by each PC. **b** PCA score plots of transcriptomes in Gly_{15} and SW_{15} PCA score plots. **c** Heatmap on the left shows the contribution of each functional category to PC1. On the right-hand side, the proportion of up- or down-regulated genes compared to Gly_{15} is given for each functional category. **d** Normalized expression counts of the top 50 annotated genes contributing the most to PC1. The heatmap represents row-standardized z-scores

2 fatty acid synthases subunits (α: *rtg127*; β: *rtg204*) (Fig. 5) and 9 other enzymes related to glycerolipids, phospholipids and carotenoid production (Additional file 1: Table S3) are upregulated in sweetwater. This is consistent with a higher lipid accumulation in SW_{15}, which is not observed in Gly_{15}. This may be explained by higher expression of β-oxidation in Gly_{15} than in SW_{15}. This process can release peroxisomal acetyl-CoA, which in turn supplies the glyoxylate cycle and potentially counteracts the ICDH-induced decline in the Krebs cycle, thus blocking the re-direction of citrate towards lipid production (Fig. 5). Therefore, cells likely produce energy by redirecting acetyl-CoA flux towards TCA cycle in Gly_{15}. In SW_{15}, reduced expression of β-oxidation related proteins such as acyl-CoA dehydrogenase (*rtg5452*), carnitine o-acyltransferase (*rtg4139*), and malate synthase (*rtg2130*), a key enzyme of the glyoxylate cycle, supports our hypothesis.

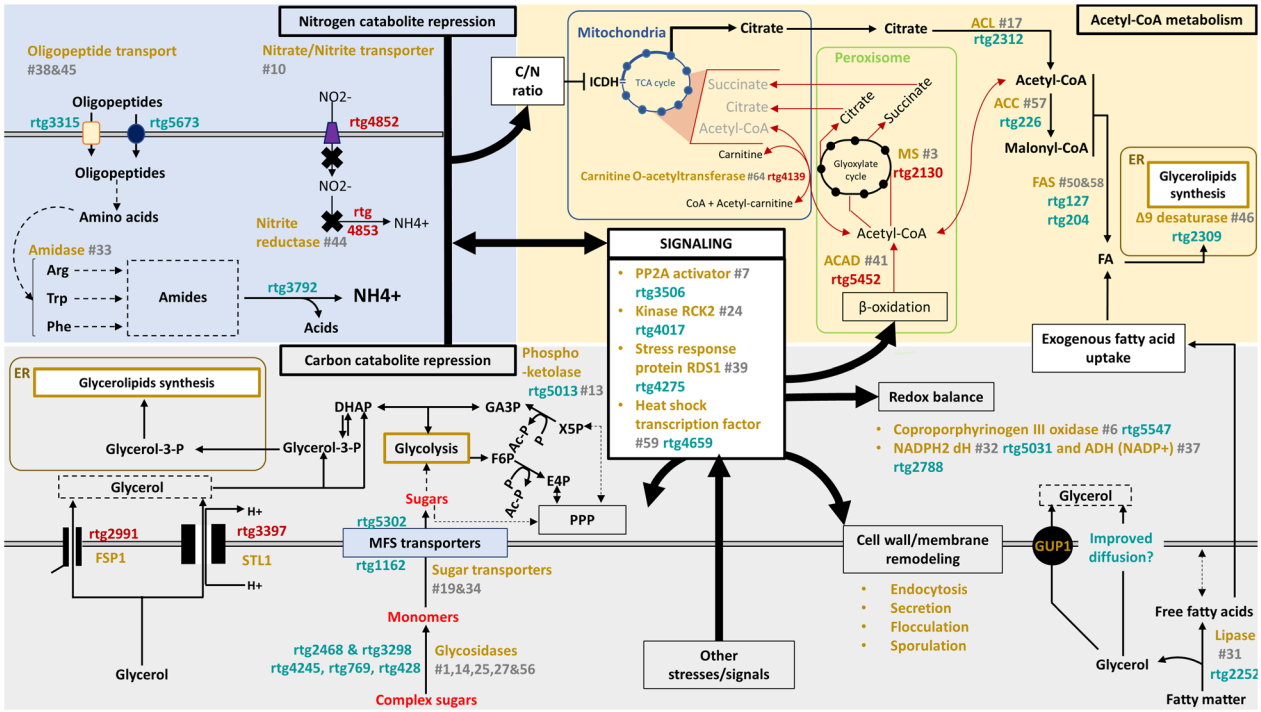

Fig. 5 Scheme summarizing the main differences between the growths of *R. toruloides* NRRL Y-6987 in SW_{15} and in Gly_{15}. Genes upregulated in SW_{15} (Gly_{15} as control) are annotated in teal while genes downregulated in SW_{15} (Gly_{15} as control) are annotated in crimson. The function or enzyme names are shown in yellow, followed by its rank in terms of contribution to PC1, shown in grey. A dashed arrow represents a potential relation, while solid lines signify a high level of confidence. *ACAD* acyl-CoA dehydrogenase, *ACC* acetyl-CoA carboxylase, *ACL* ATP citrate lyase, *ADH* alcohol dehydrogenase, *Ac-P* acetyl-phosphate, *dH* dehydrogenase, *DHAP* dihydroxyacetone, *ER* endoplasmic reticulum, *E4P* erythrose-4-phosphate, *FAS* fatty acid synthase, *F6P* fructose-6-phosphate, *GA3P* glyceraldehyde-3-phosphate, *ICDH* isocitrate dehydrogenase, *MFS* major facilitator superfamily, *MS* malate synthase, *P* phosphate, *PPP* pentose phosphate pathway, *PP2A* protein phosphatase 2A, *RCK* radiation sensitivity complementing kinase, *RDS* regulator of drug sensitivity, *X5P* xylulose-5-phosphate

Other than the presence of nitrogen source, SW_{15} also includes some tri-/di-/mono-glycerides and free fatty acids, which are by-products of fat splitting process. These components serve as potential secondary carbon sources or can be internalized to enhance the lipid content of the strain. β-Oxidation-related genes were less active in SW_{15} (Additional file 1: Table S2), but the higher expression of the 6 lipases (Additional file 1: Table S3), especially *rtg2252* confirms a possible fatty acid degradation. This hints at the incorporation of exogenous fatty acids, which bypass β-oxidation and likely directly integrate into the cellular fatty acid pool through de novo lipid accumulation, contributing to an increase of lipid content. In fact, exogenous fatty acids contribute to upregulate Δ9 desaturase in *S. cerevisiae* [35], consistent with the higher regulation of *rtg2309* (Δ9 desaturase) in SW_{15} (Fig. 5). Furthermore, genes in "intracellular trafficking, secretion, and vesicular transport" are also upregulated, indicating active secretion/externalization activities in SW_{15}. Fatty acids influx remain elusive, and it may occur via endocytosis, supported by the upregulation of *rtg1123* and *rtg2052* which encodes SLA1 and EPS15, proteins from the PAN1 complexes (Additional file 1: Table S1), which is involved in internalization of endosomes during actin-coupled endocytosis [36], possibly for incorporation of exogenous element and rapid modification of cell membrane as a response to stress [37].

Moreover, we also found the possibility of sugar utilization in SW_{15}, as glucosidases including *rtg4245* and *rtg428*, β-fructofuranosidase (*rtg769*) and glycolytic enzymes including putative rhamnogalacturonase (*rtg2468*) as well as a member of the glycosyl hydrolase family 88 (*rtg3298*) were upregulated. Among them, oligo-1,6-glucosidase (*rtg4245*) and β-fructofuranosidase (*rtg769*) were significantly upregulated, hence contributing the most to PC1 (Additional file 1: Table S2). In addition, two MFS sugar transporters (*rtg1162* and *rtg5302*) were also upregulated. Simultaneously, *rtg2991* (FSP1) and *rtg3397* (STL1) responsible for glycerol uptake were downregulated, suggesting carbon catabolite repression [38]. In terms of signaling, the most significant contrast between SW_{15} and Gly_{15} is observed in rtg3506, the activator of protein phosphatase 2A (PP2A), which

exhibits a 16.5-fold higher expression level in SW_{15}. This gene belongs to the phosphotyrosyl phosphatase activator (PTPA) family, known to promote PP2A activity. PP2A works in conjunction with the TORC pathway in yeast nitrogen sensing, but can also influence other cellular processes [39]. Hence, it is possible that TORC pathway is related to the upregulation of the genes involved in nitrogen recovery. The activation of β-oxidation by TORC is known as a response to nitrogen limitation [40], and has also been reported in *R. toruloides* [41].

Lastly, differences between SW_{15} and Gly_{15} may be influenced by pathways associated with cellular stress responses. Notably, there is an elevated expression of rtg4017 (RCK2), a gene known to be targeted by the high-osmolarity glycerol (HOG) pathway and involved in responding to both oxidative and osmotic stress [42]. Additionally, the upregulation of *rtg4275* (RDS1) associated with stress response [43], further suggests the involvement of stress-related pathways. In fact, both *rtg4017* and *rtg4275* have the highest expression in SW_{15}, consistent with the associated lower biomass production. SW_{15} may also promote adaptive mechanisms, implying that the absence of a stress response in Gly_{15} could be attributed to the cells entering a dormant or quiescent state.

Conclusions

Utilization of crude sweetwater as a feedstock was evaluated for 21 lipid-accumulating yeasts. Improved growth was achieved by diluting and supplementing nutrients, but certain strains showed better lipid accumulation with crude sweetwater. Transcriptomics analysis of *R. toluroides* NRRL Y-6987, a top-performing strain, revealed a favorable nutrient condition in sweetwater for lipid accumulation. This study demonstrated the potential of sweetwater as a feedstock for microbial oil production, suggesting *R. toluroides* NRRL Y-6987 as a promising microbial oil producer. Insights obtained regarding key mechanisms of lipid accumulation induced by sweetwater also serve as a foundation for bioprocess optimization and strain engineering.

Materials and methods

Media and sweetwater formulation

Actively growing cultures and pre-cultures were prepared using YM agar plates (containing 20 g/L agar, 3 g/L yeast extract, 3 g/L malt extract, 5 g/L peptone, and 10 g/L glucose) and YPD broth (containing 10 g/L yeast extract, 20 g/L peptone, and 20 g/L glucose). Glycerol-based defined media consist of the following components: 1.9 g/L Yeast Nitrogen Base (Formedium, CYN0501), 0.79 g/L complete supplement mixture (Formedium, DSC0019), an appropriate amount of ammonium sulfate to achieve an C/N molar ratio of 60, and glycerol at concentrations of 15, 20, 80, or 160 g/L, along with a separate 150 g/L glycerol medium prepared without additional nutrients, using ultrapure water and microbiology-grade glycerol. All media were sterilized by autoclaving prior to use. Croda (Hull, UK) supplied batches of sweetwater. The most unrefined form of sweetwater is SW_{15}, with a glycerol content of 15% (w/v) and pH of 3.9 ± 0.1 @ 20 °C, primarily attributed to free fatty acids present in sweetwater. Additionally, it contains a significant quantity of brownish fatty residues, captured by filters during sweetwater clarification process (Additional file 1: Fig. S1). SW_{35} also exhibits similar properties. When collected further down the glycerol refining process, sweetwater becomes purer but also exhibits higher alkalinity, featuring a glycerol content of 85% (w/v). Solid residues were removed by filtration prior to sweetwater use to prevent interference with optical density readings. Filtered sweetwater was further steam sterilized to avoid microbial contamination. To evaluate the pH effect, 1 M sodium hydroxide was added to SW_{15} to increase the pH to 6 ± 0.1 (@ 20 °C). To prepare $SW_{1.5}$SC medium, sterile SW_{15}, SW_{35} or SW_{85} was diluted with 2× SC nutrient mix (3.8 g/L Yeast Nitrogen Base, 1.58 g/L complete supplement mixture and 1.44 g/L ammonium sulfate) and ultrapure water. SW_{35}SC was prepared by directly dissolving 1.9 g/L Yeast Nitrogen Base, 0.79 g/L complete supplement mixture and 0.72 g/L ammonium sulfate in SW_{35}. The media was then autoclaved.

Yeast strains, cultivation conditions and growth monitoring

Yeast strains employed in this study can be found in Table 1. NRRL strains were obtained from the Agricultural Research Service (ARS) culture collection (Beltsville, USA), DSM strains from the Deutsche Sammlung von Mikroorganismen und Zellkulturen (DMSZ, Braunschweig, Germany), and BCC strains were provided by Dr. Pornkamol Unrean from BIOTEC, Thailand [44]. Cells were cultivated in a sterile environment. Strains were streaked onto YM agar plates and allowed to grow at 25 °C until colonies reached approximately 2 mm. Plates were then stored at 4 °C for a month. To prepare inoculations, a single colony was transferred into an appropriate volume of YPD, followed by incubation at 25 °C (210 rpm) until early saturation. To compare growth, an appropriate amount of inoculum and fresh media were transferred into 96-well clear U-bottom polypropylene microtiter plates (Thermo Fisher Scientific) in 4 replicates, aiming for an initial OD_{600} of 0.3. Subsequently, Inoculated plates

were sealed and placed in Titramax 1000 (Heidolph) at 25 °C and 1050 rpm for cultivation. To monitor the cultures, a SpectraMax M2e reader (Molecular Devices) was employed to measure absorbance of the cultures at 600 nm (OD_{600}) at specified time intervals. Blank correction was applied to recorded OD_{600}. Outliers due to experimental error were excluded to mitigate potential biases. Then, kinetic parameters were subsequently determined individually for each replicate using Growthcurver [45] and were used for statistical analysis. To compare over 2 conditions, ANOVA was first performed, followed by Tukey's post-hoc test or t-test. For lipid and transcriptomic analysis, cells were washed twice and suspended in 50-mL centrifuge tubes containing 5 mL of medium or 250-mL flasks containing 50 mL of medium. Cultivation was initiated with OD_{600} of 0.3 and cultures were incubated at 25 °C (210 rpm). OD_{600} was monitored using BioPhotometer Plus spectrometer (Eppendorf).

Nile red staining

250 µL to 750 µL of cell culture (depending on the cell density) were collected at target time points. Cells were harvested and washed twice with PBS pH 7 ± 0.1 @ 20 °C (1.23 g/L monobasic potassium phosphate, 0.416 g/L dibasic sodium phosphate, 8 g/L sodium chloride and 0.201 g/L potassium chloride). Washed pellets were stored at − 80 °C for further use. Frozen pellets were thawed on ice and resuspended in PBS to reach an OD_{600} of 5. 17 µL of freshly prepared DMSO:PBS (1:1) solution, 166 µL of cells suspensions (or PBS as blank) and 17 µL of freshly prepared Nile Red in acetone (60 µg/mL) were added to a black 96-well clear flat-bottom polystyrene microtiter plate (Grenier Bio-One). Four technical replicates were created for each sample and blank. Fluorescence was measured over a time course of 30 min, using excitation wavelength of 489 nm and emission wavelengths of 535 nm and 625 nm. Only fluorescence readings at 625 nm are presented. The fluorescence intensities were blank corrected and normalized with the OD_{600} of the cell suspension used. For time-course monitoring of lipid accumulation, average and standard deviations from technical replicates were depicted using GraphPad Prism. Statistical comparisons were done using ANOVA, and Tukey's post-hoc test was performed when applicable.

Neutral lipids extraction and thin layer chromatography (TLC)

Rhodosporidium toruloides NRRL Y-6987 was cultivated in 250-mL flasks containing SW_{15} and $SW_{1.5}SC$ for 4 and 10 days. Cells from a 50-mL culture were then collected through centrifugation (12 min, 3000×*g*, 4 °C), and the resulting pellets were stored at − 80 °C. Lipid extraction and TLC were performed according to previously described procedure [46]. Pellets were thawed and vortexed for 1 min. Subsequently, 775 mg from each pellet was transferred into a sterile 50-mL polypropylene centrifuge tube (Thermo Fisher Scientific). 3 mL of HCl (1 M) was added to each tube for cell hydrolysis. Mixtures were subjected to vortexing for 1 min before incubation (2-h) at 78 °C using a dry bath (Starlab). Mixtures were vortexed once for 1 min every 30 min at room temperature during incubation. After hydrolysis, cellular material was transferred into separating funnels and water was added to reach a final volume of 10 mL, followed by addition of an equal volume of chloroform/methanol mixture (1:1). Funnels were vigorously shaken, and the upper phase was removed after phase separation. The lower phase was subsequently washed with 10 mL of 0.1% (w/v) NaCl. The resulting upper phase was again removed after phase separation, and 10 mL of MilliQ water was used to wash the lower phase. After phase separation, target fractions were moved into 10-mL glass vials and dried at 65 °C for 2–3 h using a dry bath (Starlab). Dried extracts were resuspended in 500 µL of hexane and transferred into 5-mL dark glass vials and stored at − 20 °C. Five µL samples were blotted onto TLC silica gel 60 F_{254} plates (Merck). Plates were developed in pre-saturated chambers using mobile phase of a mixture of hexane: diethyl ether: acetic acid (70:30:1). After development, plates were removed from the chamber and left to dry at room temperature. Spots were then developed by immersion in a *p*-anisaldehyde solution made from 300 mL of 95% (v/v) EtOH, 12 mL of *p*-anisaldehyde, 6 mL of glacial acetic acid and 12 mL of concentrated sulfuric acid, followed by heat gun drying. Erucic acid in EtOH (10 mg/mL) and a high erucic acid rapeseed (HEAR) oil splitting product in EtOH (20 mg/mL) were used as standards.

RNA extraction and sequencing

Rhodosporidium toruloides NRRL Y-6987 were grown in SW_{15}, Gly_{15}, $SW_{1.5}SC$ and $Gly_{1.5}SC$. The first two media contained 15% (w/v) glycerol, and the latter two 1.5% (w/v) glycerol with nutrient supplementation. Three aliquots of 10 mL of culture at mid-exponential phase were harvested by centrifugation for 5 min. The specific sampling times for each medium are as follows: 61.89 h for SW_{15}, 121.1 h for Gly_{15}, 37.44 h for $SW_{1.5}SC$, and 73.85 h for $Gly_{1.5}SC$. Cells were then suspended in 1 mL of RNA*later*™ (Thermo Fisher Scientific) to stabilize the RNA, and mixed using a tube rotator for 1 h at 4 °C. Cells were then centrifuged for 5 min, and resulting pellets were stored at − 80 °C. To dilute RNA*later* and aid cell sedimentation, 14 mL of sterile DEPC-treated

ultrapure water was added. To ensure an RNAase-free environment, we utilized RNAase-free tips and tubes, and decontaminated surfaces (including the biosafety cabinet, bottles, and pipettes) using RNaseZAP (Thermo Fisher Scientific) in accordance with the manufacturer's guidelines. After thawing pellets on ice, they were resuspended in 1 mL of TRIzol reagent (Thermo Fisher Scientific). Suspensions were then moved into tubes with 250 µL of chilled, acid-washed glass beads (425–600 µm) (Sigma). Next, tubes were vortexed for 15 s and submitted to cell disruption for 15-min at 4 °C using a TissueLyser II (Qiagen) at 30 Hz. Tubes were then centrifuged for 5 min at 4 °C. Resulting supernatants were transferred to new tubes, and 200 µL of chloroform was added. After vortexing for 15 s, the solution was incubated for 5 min at room temperature. RNA extraction was conducted in accordance with manufacturer's guidelines. The resulting extracts were resuspended in 50 µL RNAse-free water and underwent DNA removal using the Turbo DNase kit (Invitrogen). Lastly, samples were concentrated through ethanol precipitation following previously outlined protocol [47], and resuspended in RNAse-free water to a final volume of 30 µL. Sample concentration and purity were monitored by NanoDrop 2000 (Thermo Fisher Scientific) at all steps. Quality of extracted RNA was assessed by electrophoresis on 1.5% (w/v) agarose gels. Prior to library preparation, the quality of the extracts was verified using the 2100 Bioanalyzer (Agilent) and NanoDrop 2000. Subsequently, PolyA enrichment, cDNA library construction, paired-end sequencing using an Illumina NovaSeq with 150 bp read length, quality control, and sequence trimming were conducted by NovogeneAIT.

Transcriptomic analysis

Trimmed reads were aligned to *R. toruloides* NRRL Y-1091 genome (NCBI GenBank accession number: GCA_001542305.1) using STAR v2.7.7 [48]. Subsequently, RSEM v1.3.3 [49] was used to quantify gene expression levels with reference to genome annotation generated by AUGUSTUS v3.3.3 [50]. Expression levels are quantified in counts of Fragments Per Kilobase of transcript per Million mapped reads (FPKM) or Transcripts Per Million (TPM). Counts processing and differential expression analysis were performed using DEseq2 v1.30.0 [51]. Initially, data filtering was done by retaining genes with TPM above 10 in at least three samples. Filtered data was normalized to adjust for variations in sequencing depth through variance stabilizing transformation [52]. Hierarchical clustering and principal component analysis utilized the normalized data, whereas TPM values were employed for DE. Significantly differentially expressed genes were defined as genes with an adjusted p-value less than 0.01. In the case of PCA and hierarchical clustering, biological replicates were not combined. Instead, the z-scores of normalized counts for pertinent genes across various conditions were utilized to assess inter-replicate variability.

Genomic analysis

We identified genes associated with glycerol metabolism, transport, and lipid biosynthesis through functional annotations, KO numbers [53] and by searching for homologous genes in other yeast species using the AYbRAH database [54]. To identify common responsive elements in the promoters of relevant genes, 1000 bp upstream and downstream of coding sequences were extracted using the FlankBed and GetFastaBed (Bedtools) [55] from GALAXY server [56]. Promoter sequences (upstream or downstream) were selected based on the gene orientation and compared in search for common motifs using info-Gibbs [57]. Identified motifs were compared to *S. cerevisiae* as well as fungal responsive element and cross-checked using compare-matrices and matrix-scan from the Regulatory Sequence Analysis Tools, respectively [58].

Supplementary Information

The online version contains supplementary material available at https://doi.org/10.1186/s12934-024-02336-x.

Additional file 1: Figure S1. Aspect and properties of the three types of sweetwater used in this study. The asterisk indicates that SW_{85} was diluted before pH measurement. **Figure S2.** Bar graphs of data shown in Table 2. Error bars indicate standard deviations. **Figure S3.** Evaluating the glycerol tolerance of oleaginous yeasts Cells were grown in 96-well microplates containing either refined glycerol diluted with synthetic complete nutrient mix for a final glycerol concentration of 2% (w/v) [black line: Gly_2SC], 8% (w/v) [blue line: Gly_8SC] or 16% (w/v) [red line: $Gly_{16}SC$]. Cells were grown in quadruplicates and the averages OD600 and associated standard deviations were plotted against time. **Figure S4.** Bar graphs of data comparing growth in $SW_{35>1.5}C$ and $SW_{35}SC$ shown in Table 3. Error bars indicate standard deviations. **Figure S5.** Bar graphs of data comparing pH 6.09 and pH 3.95 in SW_{15} shown in Table 3. Error bars indicate standard deviations. **Figure S6.** Evaluating growth in different type of sweetwater diluted with the synthetic complete nutrient mic. Cells were grown in 96-well microplates containing either in SW_{15} [black line: $SW_{15>1.5}SC$], SW_{35} [teal line: $SW_{35>1.5}SC$] or SW_{85} [purple line: $SW_{85>1.5}SC$] diluted in synthetic complete nutrient mix for a final glycerol concentration of 1.5% (*w/v*). Cells were grown in quadruplicates and the averages OD_{600} and associated standard deviations were plotted against time. **Figure S7.** Evaluating effect of sweetwater pH on growth. Cells were grown in 96-well microplates containing either sweetwater with a 15% (*w/v*) glycerol content at native pH [black line: SW_{15} pH 3.95] or sweetwater with a 15% (*w/v*) glycerol content with a pH adjusted to 6 [teal line: SW_{15} pH 6.09]. Cells were grown in quadruplicates and the averages OD_{600} and associated standard deviations were plotted against time. **Figure S8.** Clustergram of sample-to-sample Euclidean distances based on expression counts normalized by variance stabilizing transformation. **Figure S9.** Growth curves of *R. toruloides* NRRL Y-6987 in the 4 media used for the transcriptomic analysis. **Table S1.** Annotation of genes represented in the Fig. 3. **Table S2.** Top 50 of annotated genes contributing the most to PC1 in the differential expression analysis of SW_{15} vs Gly_{15}. Gene ranks in terms of contribution to PC1 were given in column Rank #, and

genes were sorted by descending contribution in each category. The smallest rank corresponds to the highest the contribution. LFC (Log2 fold change) gives the estimated change between gene expression level of in SW_{15} compared to Gly_{15} (Ctrl). This change is associated with a FDR adjusted p-value either non-significant (ns), non-computed (na), lower than 0.01 (< 0.01), between 0.01 and 0.05 (< 0.05) or between 0.05 and 0.1 (< 0.1). Only padj < 0.01 were considered significant in the manuscript.
Table S3. Differential expression results of SW_{15} vs. Gly_{15} of relevant genes associated with lipid metabolism. Gene ranks in terms of contribution to PC1 were given in column Rank # and genes were sorted by descending contribution in each category. LFC (Log2 fold change) gives the estimated change between gene expression level of in SW_{15} compared to Gly_{15} (Ctrl). This change is associated with a FDR adjusted p-value either non-significant (ns), non-computed (na), lower than 0.01 (< 0.01), between 0.01 and 0.05 (< 0.05) or between 0.05 and 0.1 (< 0.1). Only padj < 0.01 were considered significant in the manuscript.

Acknowledgements
We thank Dr. Pornkamol Unrean (BIOTEC, Thailand) for providing oleaginous yeast strains. The authors express their gratitude to the University of Sheffield Institutional Open Access Fund for providing financial support. For the purpose of open access, the author has applied a Creative Commons Attribution (CC BY) license to any Author Accepted Manuscript version arising.

Author contributions
Conceptualization: KLT, TSW and D-YL; formal analysis: VMK, YQL, ML, KLT, TSW and D-YL; investigation: VMK, DS-WO, PS, JS and IS; resources: PS, JS, and IS; writing—original draft: VMK and YQL; writing—review and editing: ML, TSW and D-YL; supervision: TSW and D-YL; funding acquisition: D-YL; All authors read and approved the final manuscript.

Funding
The research was supported by the Korea Innovation Foundation grant (2021-DD-UP-0369) funded by Ministry of Science and ICT and the Korea Institute of Planning and Evaluation for Technology in Food, Agriculture, Forestry and Fisheries (iPET) through High Value-added Food Technology Development Program (32136-05-1-HD050) funded by the MAFRA. VMK was supported by the Sheffield-A*STAR Ph.D. scholarship. This work was also supported by the Agency for Science, Technology and Research (A*STAR), Singapore, under the A*STAR Core – Central Funds (Project No: C2333017002, SIBER 2.0).

Availability of data and materials
The datasets used and/or analyzed during the current study are available from the corresponding author on reasonable request.

Declarations

Ethics approval and consent to participate
Not applicable.

Consent for publication
Not applicable.

Competing interests
The authors declare that they have no competing interests.

Author details
[1]Department of Chemical & Biological Engineering, University of Sheffield, Sir Robert Hadfield Building, Mappin Street, Sheffield S1 3JD, UK. [2]Bioprocessing Technology Institute, Agency for Science, Technology and Research (A*STAR), 20 Biopolis Way, Centros, Singapore 138668, Singapore. [3]School of Chemical Engineering, Sungkyunkwan University, 2066 Seobu-ro, Jangan-gu, Suwon, Gyeonggi-do 16419, Republic of Korea. [4]Department of Biotechnology, Bhupat and Jyoti Mehta School of Biosciences, Indian Institute of Technology Madras, Chennai 600036, India. [5]Croda Europe Ltd., Oak Road, Clough Road, Hull HU6 7PH, UK. [6]Evolutor Ltd, The Innovation Centre, 217 Portobello, Sheffield S1 4DP, UK. [7]National Center for Genetic Engineering and Biotechnology, 113 Thailand Science Park, Phahonyothin Road, Khlong Nueang, Khlong Luang 12120, Pathum Thani, Thailand. [8]School of Pharmacy, Bandung Institute of Technology, 10 Coblong, Bandung, West Java 40132, Indonesia.

Received: 27 October 2023 Accepted: 14 February 2024
Published online: 24 February 2024

References

1. Kaur J, Sarma AK, Jha MK, Gera P. Valorisation of crude glycerol to value-added products: perspectives of process technology, economics and environmental issues. Biotechnol Rep. 2020;27: e00487.
2. Luo X, Ge X, Cui S, Li Y. Value-added processing of crude glycerol into chemicals and polymers. Bioresour Technol. 2016;215:144–54.
3. González-Villanueva M, Galaiya H, Staniland P, Staniland J, Savill I, Wong TS, et al. Adaptive laboratory evolution of *Cupriavidus necator* H16 for carbon co-utilization with glycerol. Int J Mol Sci. 2019;20:5737.
4. Tomás-Pejó E, Morales-Palomo S, González-Fernández C. Microbial lipids from organic wastes: outlook and challenges. Bioresour Technol. 2021;323: 124612.
5. Thevenieau F, Nicaud JM. Microorganisms as sources of oils. OCL Oilseeds Fats Crop Lipids. 2013;20:603.
6. Gao Z, Ma Y, Wang Q, Zhang M, Wang J, Liu Y. Effect of crude glycerol impurities on lipid preparation by *Rhodosporidium toruloides* yeast 32489. Bioresour Technol. 2016;218:373–9.
7. Samul D, Leja K, Grajek W. Impurities of crude glycerol and their effect on metabolite production. Ann Microbiol. 2014;64:891–8.
8. Muniraj IK, Uthandi SK, Hu Z, Xiao L, Zhan X. Microbial lipid production from renewable and waste materials for second-generation biodiesel feedstock. Environ Technol Rev. 2015;4:1–16.
9. Ito T, Nakashimada Y, Senba K, Matsui T, Nishio N. Hydrogen and ethanol production from glycerol-containing wastes discharged after biodiesel manufacturing process. J Biosci Bioeng. 2005;100:260–5.
10. Signori L, Ami D, Posteri R, Giuzzi A, Mereghetti P, Porro D, et al. Assessing an effective feeding strategy to optimize crude glycerol utilization as sustainable carbon source for lipid accumulation in oleaginous yeasts. Microb Cell Fact. 2016;15:1–19.
11. Ciriminna R, Pina CD, Rossi M, Pagliaro M. Understanding the glycerol market. Eur J Lipid Sci Technol. 2014;116:1432–9.
12. Pagliaro M. Glycerol: the renewable platform chemical. Amsterdam: Elsevier; 2017.
13. Keita VM, Gonzalez-Villanueva M, Wong TS, Tee KL. Microbial utilization of glycerol for biomanufacturing. In: Engineering of microbial biosynthetic pathways. Singapore: Springer; 2020. p. 245–302.
14. Mota CJA, Peres Pinto B, de Lima AL. Glycerol utilization. In: Glycerol. Cham: Springer; 2017. p. 11–9.
15. Mota MN, Múgica P, Sá-Correia I. Exploring yeast diversity to produce lipid-based biofuels from agro-forestry and industrial organic residues. J Fungi. 2022;8:687.
16. Chattopadhyay A, Maiti MK. Lipid production by oleaginous yeasts. Adv Appl Microbiol. 2021;116:1–98.
17. Chiruvolu V, Eskridge K, Cregg J, Meagher M. Effects of glycerol concentration and pH on growth of recombinant *Pichia pastoris* yeast. Appl Biochem Biotechnol Part A Enzym Eng Biotechnol. 1998;75:163–73.
18. Swinnen S, Klein M, Carrillo M, McInnes J, Nguyen HTT, Nevoigt E. Re-evaluation of glycerol utilization in *Saccharomyces cerevisiae*: characterization of an isolate that grows on glycerol without supporting supplements. Biotechnol Biofuels. 2013;6:1–12.
19. Tan HW, Abdul Aziz AR, Aroua MK. Glycerol production and its applications as a raw material: a review. Renew Sustain Energy Rev. 2013;27:118–27.
20. Yoshino M, Murakami K. AMP deaminase reaction as a control system of glycolysis in yeast. Activation of phosphofructokinase and pyruvate kinase by the AMP deaminase-ammonia system. J Biol Chem. 1982;257:2822–8.
21. Adrio JL. Oleaginous yeasts: promising platforms for the production of oleochemicals and biofuels. Biotechnol Bioeng. 2017;114:1915–20.

22. Botham PA, Ratledge C. A biochemical explanation for lipid accumulation in Candida 107 and other oleaginous micro-organisms. J Gen Microbiol. 1979;114:361–75.
23. Patel A, Matsakas L. A comparative study on de novo and ex novo lipid fermentation by oleaginous yeast using glucose and sonicated waste cooking oil. Ultrason Sonochem. 2019;52:364–74.
24. Matatkova O, Gharwalova L, Zimola M, Rezanka T, Masak J, Kolouchova I. using odd-alkanes as a carbon source to increase the content of nutritionally important fatty acids in *Candida krusei*, *Trichosporon cutaneum*, and *Yarrowia lipolytica*. Int J Anal Chem. 2017;2017:8195329.
25. Beopoulos A, Mrozova Z, Thevenieau F, Le Dall MT, Hapala I, Papanikolaou S, et al. Control of lipid accumulation in the yeast *Yarrowia lipolytica*. Appl Environ Microbiol. 2008;74:7779–89.
26. Ratledge C. Microbial oils: an introductory overview of current status and future prospects. OCL Oilseeds Crop Fats Lipids. 2013;20:602.
27. Schulze I. Microbial lipid production with oleaginous yeasts. 2014.
28. Buck JW, Andrews JH. Attachment of the yeast *Rhodosporidium toruloides* is mediated by adhesives localized at sites of bud cell development. Appl Environ Microbiol. 1999;65:465–71.
29. Chambers P, Issaka A, Palecek SP. *Saccharomyces cerevisiae* JEN1 promoter activity is inversely related to concentration of repressing sugar. Appl Environ Microbiol. 2004;70:8–17.
30. Boeckstaens M, André B, Marini AM. The yeast ammonium transport protein Mep2 and its positive regulator, the Npr1 kinase, play an important role in normal and pseudohyphal growth on various nitrogen media through retrieval of excreted ammonium. Mol Microbiol. 2007;64:534–46.
31. Crépin L, Sanchez I, Nidelet T, Dequin S, Camarasa C. Efficient ammonium uptake and mobilization of vacuolar arginine by *Saccharomyces cerevisiae* wine strains during wine fermentation. Microb Cell Fact. 2014;13:1–13.
32. Beltran G, Novo M, Rozès N, Mas A, Guillamón JM. Nitrogen catabolite repression in *Saccharomyces cerevisiae* during wine fermentations. FEMS Yeast Res. 2004;4:625–32.
33. Banks GR, Shelton PA, Kanuga N, Holden DW, Spanos A. The *Ustilago maydis* nar 1 gene encoding nitrate reductase activity: sequence and transcriptional regulation. Gene. 1993;131:69–78.
34. Johns AMB, Love J, Aves SJ. Four inducible promoters for controlled gene expression in the oleaginous yeast *Rhodotorula toruloides*. Front Microbiol. 2016;7: 225256.
35. Bossie MA, Martin CE. Nutritional regulation of a yeast Δ-9 fatty acid desaturase activity. J Bacteriol. 1989;171:6409–13.
36. Martin R, Hellwig D, Schaub Y, Bauer J, Walther A, Wendland J. Functional analysis of *Candida albicans* genes whose *Saccharomyces cerevisiae* homologues are involved in endocytosis. Yeast. 2007;24:511–22.
37. López-Hernández T, Haucke V, Maritzen T. Endocytosis in the adaptation to cellular stress. Cell Stress. 2020;4:230–47.
38. Bommareddy RR, Sabra W, Zeng AP. Glucose-mediated regulation of glycerol uptake in *Rhodosporidium toruloides*: insights through transcriptomic analysis on dual substrate fermentation. Eng Life Sci. 2017;17:282–91.
39. Ariño J, Velázquez D, Casamayor A. Ser/thr protein phosphatases in fungi: structure, regulation and function. Microb Cell. 2019;6:217–56.
40. Gossing M, Smialowska A, Nielsen J. Impact of forced fatty acid synthesis on metabolism and physiology of *Saccharomyces cerevisiae*. FEMS Yeast Res. 2018;18:96.
41. Zhu Z, Zhang S, Liu H, Shen H, Lin X, Yang F, et al. A multi-omic map of the lipid-producing yeast *Rhodosporidium toruloides*. Nat Commun. 2012;3:1–12.
42. Bilsland-Marchesan E, Ariño J, Saito H, Sunnerhagen P, Posas F. Rck2 kinase is a substrate for the osmotic stress-activated mitogen-activated protein kinase Hog1. Mol Cell Biol. 2000;20:3887–95.
43. Ludin KM, Hilti N, Schweingruber ME. Schizosaccharomyces pombe rds1, an adenine-repressible gene regulated by glucose, ammonium, phosphate, carbon dioxide and temperature. MGG Mol Gen Genet. 1995;248:439–45.
44. Unrean P, Champreda V. High-throughput screening and dual feeding fed-batch strategy for enhanced single-cell oil accumulation in *Yarrowia lipolytica*. Bioenergy Res. 2017;10:1057–65.
45. Sprouffske K, Wagner A. Growthcurver: an R package for obtaining interpretable metrics from microbial growth curves. BMC Bioinform. 2016;17:1–4.
46. Sobus MT, Holmlund CE. Extraction of lipids from yeast. Lipids. 1976;11:341–8.
47. Green MR, Sambrook J. Precipitation of DNA with ethanol. Cold Spring Harb Protoc. 2016;2016:1116–20.
48. Dobin A, Davis CA, Schlesinger F, Drenkow J, Zaleski C, Jha S, et al. STAR: ultrafast universal RNA-seq aligner. Bioinformatics. 2013;29:15–21.
49. Li B, Dewey CN. RSEM: accurate transcript quantification from RNA-Seq data with or without a reference genome. BMC Bioinform. 2011;12:1–16.
50. Stanke M, Morgenstern B. AUGUSTUS: a web server for gene prediction in eukaryotes that allows user-defined constraints. Nucleic Acids Res. 2005;33:W465–7.
51. Love MI, Huber W, Anders S. Moderated estimation of fold change and dispersion for RNA-seq data with DESeq2. Genome Biol. 2014;15:1–21.
52. Anders S, Huber W. Differential expression analysis for sequence count data. Genome Biol. 2010;11:1–12.
53. Mao X, Cai T, Olyarchuk JG, Wei L. Automated genome annotation and pathway identification using the KEGG orthology (KO) as a controlled vocabulary. Bioinformatics. 2005;21:3787–93.
54. Correia K, Yu SM, Mahadevan R. AYbRAH: a curated ortholog database for yeasts and fungi spanning 600 million years of evolution. Database. 2019;2019: baz022.
55. Quinlan AR, Hall IM. BEDTools: a flexible suite of utilities for comparing genomic features. Bioinformatics. 2010;26:841–2.
56. Giardine BM, Riemer C, Burhans R, Ratan A, Miller W. Some phenotype association tools in galaxy: looking for disease SNPs in a full genome. Curr Protoc Bioinform. 2012;39:15–22.
57. Defrance M, van Helden J. info-gibbs: a motif discovery algorithm that directly optimizes information content during sampling. Bioinformatics. 2009;25:2715–22.
58. Nguyen NTT, Contreras-Moreira B, Castro-Mondragon JA, Santana-Garcia W, Ossio R, Robles-Espinoza CD, et al. RSAT 2018: regulatory sequence analysis tools 20th anniversary. Nucleic Acids Res. 2018;46:209–14.

Publisher's Note